Dalton Transactions

Accepted Manuscript

ROYAL SOCIETY OF CHEMISTRY

www.rsc.org/dalton

DFT Study of the Interaction between Olefins and Cu^{2+} on Silica and MCM-41 Model Surfaces

Yunlong Gao[*,†] and Lowell D. Kispert[‡]

College of Science, Nanjing Agricultural University, Nanjing, 210095 China and Department of Chemistry, BOX 870336, University of Alabama, Tuscaloosa, Alabama 35487.

* To whom correspondence should be addressed. E-mail: yunlong@njau.edu.cn

† Nanjing Agricultural University.

‡ University of Alabama.

Abstract

The interaction between ethylene and Cu^{2+} on a silica model surface was studied by density functional theory (DFT) with nine popular functionals. It is found that B3LYP with BSSE correction is the best method by comparing the calculated results with reported experimental data. This method was also used to study the interactions of Cu^{2+} with β-carotene, 1,3,5,7,9,11,13-tetradecaheptaene and ethylene on a MCM-41 model surface, respectively. The relationship between the reorganization energy of an olefin and its conjugation length was studied, and the roles of the electrostatic interaction between the olefin and the Cu^{2+} were investigated. It is also found that the different environments of Cu^{2+} affect the Cu^{2+}-olefin interaction significantly.

Introduction

The metal-olefin interaction occurs in many significant chemical processes such as olefin hydro-genation, isomerization, hydrocarbonlyation, hydroformylation, polymerization, and metathesis. The metal-olefin complexes are key intermediates in these important industrial processes.[1-6] It is very important to synthesize catalysts for these reactions which are able to meet the needs of a particular reaction or process because the use of olefins and olefin-related products in industry has become prevalent. Therefore, a complete understanding of the nature of the metal-olefin bond and the factors that influence the bond strength is critical for the

synthesis of these catalysts.

The metal-olefin bonding is well described by the Dewar-Chatt-Duncanson (DCD) model, which is based on the Frontier Molecular Orbital Theory introduced by Dewar in 1951,[7] and expanded by Chatt and Duncanson in 1953.[8] The DCD model details the metal-olefin bond as being a two way synergistic electron exchange between a metal complex and an olefin. These two being: (1) σ interaction, i.e. olefin HOMO (π) donates electron density to the metal LUMO (a dsp hybrid), and (2) π bonding interaction, i.e. Metal HOMO (d-character) donates electron density to the olefin LUMO (π*). The DCD model can be used to qualitatively explain the geometrical changes in the olefin (C=C bond stretches due to back bonding and bonding from olefin substituents), olefin rotation around the metal-olefin bond axis, and the extent of the metal-olefin interaction, which can be measured as a bond strength.[9] However, the qualitative nature of this model limits the complete rationalization of metal-olefin bond strengths. According to the DCD model, it can be qualitatively predicted that the more electron withdrawing an olefin is the stronger the metal-olefin bond. However, the experimental data contradicts this prediction. For example, the metal-olefin bond strength of $Cr(CO)_5(C_2X_4)$ (X=halogen) decreases in the order: $Cr\text{-}C_2H_4 > Cr\text{-}C_2F_4 > Cr\text{-}C_2Cl_4$.[10] Clearly, the metal-olefin interaction is not only determined by the extent of orbital interactions, but other factors as well. Further studies[11-14] show that although the attractive orbital interaction between metal and the olefin increases as the olefin becomes more electron withdrawing, this bond-favoring trend is counterbalanced by the Pauli (steric) repulsion energy, which also increases as the number of electron-withdrawing substituents increases. Besides, metal-olefins bond strengths are influenced to a great extent by the deformation of the olefin in addition to the well known influence of electronic and steric effects.[11-14] Deformation of the olefin involves: elongation of the C=C bond and bending of substituents out from the C=C plane. The stronger the metal-olefin interaction, the larger the deformation of the olefin. In addition, the olefin reorganization is energetically costly, thus reducing the overall interaction energy (IE).

To extend the DCD model, more experiments and quantum mechanical calculations are needed to be carried out to account for all factors in the metal-olefin interaction. Most of the reported quantum mechanical calculations for the metal-olefin interaction were carried out by

density functional theory (DFT), which has emerged during the past decades as a powerful methodology for the simulation of chemical systems because of its good accuracy and reasonable computational cost.[11-15] In comparison with ab initio calculations, the DFT method includes electron correlation via functions and is more biased toward π-electron delocalization.[16] Therefore, DFT can perform quite satisfactorily on conjugated molecules of moderate size, such as polyenes and carotenoids. However, the accuracy of these calculations on the metal-olefin interaction is uncertain due to the lack of experimental data with which to compare, such as the geometries of the metal-olefin complexes, the interaction energies, etc. The interaction of deuterated ethylene (C_2D_4) with Cu^{2+}, which was ion-exchanged onto a silica gel, was studied by Ichlkawa et al.[17] using electron spin resonance (EPR) and electron spin echo modulation (ESEM) measurements. The Cu-D distance was accurately measured by ESEM to be 4.1 ± 0.2 Å. Further study by Narayana et al.[18] demonstrates how Cu^{2+} is introduced into a silica gel surface affect the interaction of ethylene with Cu^{2+}. For Cu^{2+} impregnated into a silica gel surface, the Cu-D distance is 3.3 ± 0.1 Å, which is much shorter than that for Cu^{2+} ion-exchanged into a silica gel surface. The difference is attributed to the different environments of Cu^{2+} on the silica surface. The interaction of per-deuterated β-carotene (**I**) (Chart 1) with Cu^{2+}, which is ion-exchanged into MCM-41 (Mobil Composition of Matter No. 41) molecular sieves, was studied by Gao et al.[19] using ESEEM (electron spin-echo envelope modulation) and pulse ENDOR (Electron Nuclear Double Resonance). It was found that Cu^{2+} interacts with the middle double bond of β-carotene, and the Cu-D distance was found to be 3.3 ± 0.2 Å. However, these studies can only provide the distances between the olefin and the metal. Other information such as the interaction energy and the reorganization energy cannot be determined, and the studies can neither tell why Cu^{2+} interacts with only the middle double bond of β-carotene nor how the conjugation length of an olefin affects the metal-olefin interaction. Besides, these experiments are difficult to carry out as the per-deuterated olefins are usually not experimentally available (the per-deuterated olefins were used in the experiments to avoid the interferences from the hydrogen atoms on the silica or MCM-41 surfaces).

In this study, the first purpose is to find out which method is suitable for the DFT study of the interaction between Cu^{2+} and the olefin. The simplest olefin ethylene was used in the

calculations, and the calculated results were compared to the experimental data to determine which functional is suitable for the DFT study. Then the DFT studies of Cu^{2+} with different olefins using the developed method were carried out to understand the Cu^{2+}-olefin interaction. A simple model for Cu^{2+} on a silica surface was built based on published studies,[17, 18, 20-22] and the interaction between Cu^{2+} and ethylene on the silica surface was studied by density functional theory (DFT). The distances between Cu^{2+} and ethylene were calculated with nine popular density functionals (B3LYP, BP86, PBEPBE, TPSSTPSS, B97D, wB97XD, M06, M06L and CAM-B3LYP), and by using, respectively, the basis set 6-311+G(d,p) and the mixed basis set 6-311+G(d,p) + LANL2DZ (on Cu^{2+}). The calculated results were compared to the reported distance measured by using electron spin echo modulation (ESEM) spectrometry.[17] It is found that B3LYP is suitable for the calculations with accuracy and cost considered, and the distance calculated by B3LYP/6-311+G(d,p) is about 0.4 Å closer to the reported data than by using the mixed basis set. The distance calculated by B3LYP with basis set superposition error (BSSE) correction is about 0.1 Å closer to the experimental value than that without the BSSE correction. The model for Cu^{2+} on a MCM-41 surface was also based on the published studies.[19,23] The interaction between Cu^{2+} and β-carotene (**I**) was calculated by B3LYP with the BSSE correction. The calculated Cu-H distance is about 3.16 Å, which is in agreement with the measured value 3.3 ± 0.2 Å by ESEEM.[19] To study how the conjugation length of an olefin affects the interaction, the interaction of Cu^{2+} with 1,3,5,7,9,11,13-tetra- decaheptaene (**II**) and ethylene (**III**), were also calculated by B3LYP with the BSSE correction, respectively, and the results were compared to those of **I**. The calculated interaction energy (IE) decreases in the order **III** > **I** > **II**, and the calculated reorganization energy of **I**, **II** and **III** decreases with the decrease of the conjugation length from **I** to **II** to **III**. Although the reorganization energy of **I** is larger than that of **II**, the interaction between **I** and Cu^{2+} is stronger than that between **II** and Cu^{2+}. This is attributed to the stronger electrostatic attraction between **I** and Cu^{2+}. The calculated charge distribution of **I** shows that more negative charge is located at the middle of **I**, which explains why Cu^{2+} prefers to interact with the middle double bond of **I**. The calculations also support the reported experimental results[17,18] which show that the different environments of Cu^{2+} affect the Cu^{2+}-olefin interaction significantly.

Computational details

All computations were performed with the Gaussian 09[24] suite of programs. The set of functionals not designed to account for dispersion includes the standard generalized gradient approximation (GGA) functionals BP86[25,26] and PBEPBE,[27,28] the hybrid-GGA functional B3LYP,[29] and the meta-GGA functional TPSSTPSS.[30] Among the functionals accounting for dispersion, both the GGA functional B97D,[31,32] and the hybrid meta-GGA functional wB97XD,[31,32] contain empirical dispersion terms, and the latter also long-range corrections. The meta-GGA (M06L) and hybrid counterpart (M06)[33,34] account for non-covalent attractions and dispersion via extensive parametrization using training sets including non-covalently bound complexes as well as transition metal energetics.[33,34] The LC-DFT method CAM-B3LYP[35] was also investigated. Calculations with basis set superposition error (BSSE) correction were carried out by the counterpoise method of Boys–Bernardi.[36] In this study, two fragment BSSE correction is used. The olefin denoted as A and the metal complex denoted as B with the Cu^{2+}-olefin complex denoted as AB.

The typical, uncorrected interaction energy between monomers A and B is computed as:

$$\Delta E_{\text{int}}(AB) = E_{AB}^{AB}(AB) - E_{A}^{A}(A) - E_{B}^{B}(B) \quad (1)$$

where the superscripts denote the basis used, the subscripts denote the geometry, and the symbol in parentheses denotes the chemical system considered. Thus, $E_{AB}^{AB}(AB)$ represents the energy of the bimolecular complex AB evaluated in the dimer basis (the union of the basis sets on A and B), computed at the geometry of the dimer. Likewise, monomers A and B are each evaluated at their own geometries in their own basis sets.

Eq. (1) can be corrected by estimating the amount by which monomer A is stabilized by the extra basis functions from monomer B (and vice versa). This may be estimated as:

$$E_{BSSE}(A) = E_{A}^{AB}(A) - E_{A}^{A}(A) \quad (2)$$

$$E_{BSSE}(B) = E_{B}^{AB}(B) - E_{B}^{B}(B)$$

where the energy of monomer A in its monomer basis is subtracted from the energy of monomer A in the dimer basis (and likewise for monomer B). The interaction energy

between A and B with BSSE correction can be obtained by subtracting this error from the interaction energy defined in Eq. 1, the terms $E_A^A(A)$ and $E_B^B(B)$ cancel, yielding:

$$\Delta E_{\text{int}}^{CP}(AB) = E_{AB}^{AB}(AB) - E_A^{AB}(A) - E_B^{AB}(B) \quad (3)$$

where "CP" stands for counterpoise.

The reorganization energy (RE) of an olefin (A) is calculated as:

$$RE(A) = E_1(A) - E_2(A) \quad (4)$$

where $E_1(A)$ is energy calculated using the geometry of A in the optimized Cu^{2+}-olefin (AB) complex, and $E_2(A)$ is the energy calculated using the optimized geometry of A in the absence of Cu^{2+} complex. For consistency's sake, the same basis set for A is used in all the calculations.

Results and discussion

The model for Cu^{2+} on a silica gel surface (Cu^{2+} is introduced onto silica surface by ion-exchange) was based on the EPR and ESEM studies by Ichikawa et al.[17,20] The silica surface features reviewed by Rimola et al.[22] was also considered in the model-building. The process for the introduction of Cu^{2+} onto a silica gel surface includes ion-exchange and thermal activation.[17,20] In the ion-exchange process, Cu^{2+} exchanges with the protons of the silanol groups (SiOH) on the silica gel surface.[17,20,37] EPR and ESEM studies show that Cu^{2+} is in a distorted tetrahedral environment coordinated to four lattice oxygens after thermal activation.[17,20] According to Rimola et al.,[22] the O and H atoms of the silanol groups (-SiOH) on a silica gel surface are flexible. Based on this information, the simple model for Cu^{2+} on a silica surface is shown in Fig. 1a, with Cu^{2+} coordinating to two OH^- and two H_2O. The geometry optimization was performed by B3LYP/6-311+G(d,p). The distance between O1 and O2 set equal to that between O3 and O4 (3.14 Å), and the distance between O2 and O3 equal to that between O1 and O4 (2.49 Å). The distance between O1 and O3 is 4.25 Å, and that between O2 and O4 is 3.71 Å. All these distances are consistent with the neighbor O-O distances on the silica surface.[22] The bond length of Cu-O1 equals to that of Cu-O3 (2.130 Å) and the bond length of Cu-O2 equals to that of Cu-O4 (1.858 Å), and these bond lengths are typical Cu-O bond lengths.[21] The distance between one proton of H_2O and the O of OH^- is

1.819 Å, and the angle ∠ O1-H-O4 or ∠O2-H-O3 is 122.6°, indicating a weak hydrogen bond. All O-O and O-H distances obtained after geometry optimization are in agreement with those on a silica surface,[22] indicating that this model is reasonable.

The geometry optimization of Cu^{2+}-C_2H_4 complex was carried out with nine functionals. The all-electron triple-ζ Pople type basis set 6-311+G(d,p), and the mixed basis set 6-311+G(d,p) + LANL2DZ, which utilizes the Los Alamos Effective Core Potential on Cu^{2+} while utilizing the Pople type basis set on all other atoms, were employed in the calculations, respectively. The Pople type split valence basis sets are extensively used in *ab initio* quantum chemistry calculations, and as a result are well validated. LANL2DZ (Los Alamos National Laboratory 2 Double-Zeta), which is a widely used ECP (effective core potential) type basis set, was used to model the metal atoms.[38] The mixed basis set has been extensively used along with density functional methods for studies of transition metal containing systems. Mixed basis sets of this type have been very popular in computational chemistry studies in this area in recent years.[39] Performances of the basis set 6-311+G(d,p) and the mixed basis set 6-311+G(d,p) + LANL2DZ were evaluated in this study. Figure 1b shows the optimized structure of the complex by B3LYP/6-311+G(d,p). The four Cu-H distances are almost the same, and the bond lengths of Cu-O1 and Cu-O2 increase slightly compared to those in Fig. 1a, indicating that the interaction of C_2H_4 with Cu^{2+} causes an increase in the Cu-O coordination bond length. Figure 2 shows the Cu-H distances (average value of the four Cu-H distances) calculated by the nine functionals using the basis set 6-311+G(d,p) and the mixed basis set 6-311+G(d,p)+LANL2DZ, respectively. For comparison, the Cu-D distance measured by ESEM is also shown in the figure. With the measured distance by ESEM as the benchmark, it is determined that B3LYP performs more accurate than other functionals by ~0.1-0.9 Å with 6-311+G(d,p) as the basis set, and B3LYP/6-311+G(d,p) performs better than B3LYP/6-311+G(d,p)+LANL2DZ by ~0.4 Å.

The B3LYP/6-311+G(d,p) method shows that the interaction of C_2H_4 with Cu^{2+} causes an increase in the Cu-O bond length. To determine whether it is true for other methods, the bond length of Cu-O1 (O1 is the oxygen in the water ligand) and that of Cu-O2 (O2 is the oxygen in the hydroxyl ligand) before and after the interaction, were calculated with the nine functionals using B3LYP/6-311+G(d,p). These are shown in Fig. 3a and Fig. 3b,

respectively. It is concluded from figure 3 that the interaction of C_2H_4 with Cu^{2+} causes an increase in the Cu-O bond length, and the largest increase occurs for M06 and M06L functionals. The bond length of Cu-O1 and that of Cu-O2 before and after the interaction of C_2H_4 with Cu^{2+}, calculated with the nine functionals using the mixed basis set 6-311+G(d,p)+LANL2DZ, are shown in Fig, S1a and b, respectively. Similar results can be obtained without the functional wB97XD, which predicts that the Cu-O1 bond length (2.558 Å) is much longer and the Cu-O2 bond length (1.798 Å) is much shorter than those calculated by other functionals before the interaction of C_2H_4 with Cu^{2+}. Since the Cu-O bond length calculated by the method wB97XD/6-311+G(d,p)+LANL2DZ is either longer or shorter than the typical Cu-O bond lengths,[21] this method is not suitable.

Although B3LYP/6-311+G(d,p) outperforms other methods by ~0.1-0.9 Å in the prediction of the Cu-H distance, the calculated value is about 0.3 Å shorter than the benchmark ESEM value. To improve the calculation accuracy, larger basis sets with an increase in the polarization and diffusion components, such as 6-311++G(2d,2p), 6-311++G(3d,3p) and 6-311++G(df,pd) were applied to the calculations. The basis set aug-cc-pVTZ, which is the correlation-consistent, polarized valence, triple-ζ basis set augmented with diffuse functions on all atoms,[40,41] was also examined. The calculated Cu-H distances with B3LYP functional using those basis sets mentioned above are similar to that by B3LYP/6-311+G(d,p) (Fig. S2), indicating that larger basis sets do not improve calculation accuracy. Since the interaction between C_2H_4 and Cu^{2+} is an intermolecular interaction, and the intermolecular distance is large, the basis set superposition error (BSSE) need be corrected. For the calculations with the BSSE correction, the counterpoise method of Boys–Bernardi[36] was applied with C_2H_4 as one fragment and the Cu^{2+} complex as another fragment. The optimized geometry of the Cu^{2+}-C_2H_4 complex by B3LYP/6-311+G(d,p) with the BSSE correction (Fig. 1c) shows that the Cu-H distance increases slightly (~0.1 Å) compared to that in Fig. 1b, and the Cu-O bond lengths are slightly shorter than those in Fig. 1b, but longer than those in Fig. 1a. The calculated Cu-H distances by B3LYP using the other larger basis sets shown in Fig. S2 are similar to that by B3LYP/6-311+G(d,p), and the values are ~0.1 Å closer to the benchmark value 4.1 ± 0.2 Å, suggesting that the BSSE correction is necessary for the Cu^{2+}-olefin complexe calculations. To determine whether the deuterated

ethylene (C_2D_4) used in the ESEM experiment behaves differently from C_2H_4 when interacting with Cu^{2+}, the optimized geometries of Cu^{2+}-C_2D_4 by B3LYP/6-311+G(d,p) with and without the BSSE correction are compared to those in Fig. 1. No difference was found. Although the Cu-H distance calculated with the BSSE correction increases only slightly (about 0.1 Å), the calculated interaction energies (IE) shown in Fig. 4 are about half of those calculated without the BSSE correction, which can be attributed to the different methods used in the calculations. The calculated IE with the BSSE calculation is only ~0.3 kcal/mol, suggesting that the interaction of C_2H_4 with Cu^{2+} is very weak on a silica surface.

ESEEM and pulse ENDOR studies[19] show that Cu^{2+} interacts with the middle C15=C15′ double bond of β-carotene (**I**) (see Chart 1) on MCM-41, and formation of the Cu^{2+}-**I** complex favors light-driven electron transfer (ET) from **I** to Cu^{2+} and also permits thermal back ET from Cu+ to $\mathbf{I}^{\bullet+}$ (radical cation of **I**).[23] To investigate why Cu^{2+} interacts with the middle C15=C15′ double bond of **I**, the Mulliken atomic charges of **I** were calculated by B3LYP/6-31G(d). Figure 5a shows the optimized structure of **I**. The charges on carbons from C5 (C5′) to C15 (C15′) listed in Table 1 show that more negative charges are located in the middle of the chain, i.e. C14, C15, C15′ and C14′. Since the charges on the hydrogen atoms of the conjugated chain are almost the same (~ 0.12) and Cu^{2+} is closer to the carbons than the hydrogen atoms connected to those carbons, the electrostatic interaction strength between Cu^{2+} and **I** depends on the charge on the carbons and the number of carbons closest to Cu^{2+}. For C5=C6 (C5′=C6′) and C7=C8 (C7′=C8′) double bonds, the steric hindrance by the terminal bulky trimethyl cyclohexene rings precludes Cu^{2+} from accessing to these double bonds. For C9=C10 (C9′=C10′) and C13=C14 (C13′=C14′) double bonds, the charges on C9 (C9′) and C13 (C13′) are positive, which repel Cu^{2+}. Although the charges on both carbons of C11=C12 (C11′=C12′) double bonds are negative, the neighbor's positive charged C13 (C13′) repels Cu^{2+}. The charges on the middle four carbons are all negative, and the charge on C14 (C14′) is much more negative than those on other carbons except for that on C7 (C7′), which explains why Cu^{2+} interacts with the middle double bond C15=C15′. The calculations (see below) also show that the interaction energy (IE) between the middle double bond and Cu^{2+} is larger than that between C11=C12 and Cu^{2+} on the MCM-41 model surface.

To study the interaction between Cu^{2+} and β-carotene (**I**), requires a model for Cu^{2+} on

the MCM-41 surface. The EPR study[23] shows that Cu^{2+} coordinates to four framework oxygen atoms and is in a distorted tetrahedral environment after Cu^{2+} is introduced onto the MCM-41 surface by an ion-exchange method. When **I** interacts with Cu^{2+}, it replaces one silanol ligand forming a tetragonal coordination.[23] Different configurations of Cu^{2+}-**I** complex were examined in the calculations, and the minimum energy configuration is shown in Fig. 5b. The optimized structure is deduced by B3LYP with the BSSE correction between 2 fragments (Cu^{2+} complex as one fragment and **I** as the other fragment), and Cu^{2+} in a tetragonal environment. Since the system is large, a combination of basis sets was implemented in order to perform efficient, yet sufficiently accurate, calculations. The mixed basis set includes 6-311+G(d) for Cu, 6-31G(d) for **I** and the three oxygen atoms coordinated to Cu^{2+}, and 3-21G for the remaining atoms. The calculated distances between Cu^{2+} and the two hydrogen atoms at the middle chain are almost the same, and the average Cu-H distance is about 3.16 Å, which fits very well with the measured value 3.3 ± 0.2 Å by ESEEM.[19] This supports the previous conclusion that B3LYP with the BSSE correction is suitable for the Cu^{2+}-olefin interaction. The calculated IE is -2.61 kcal/mol. Figure S3 shows the optimized geometry of Cu^{2+}-**I** with the C11=C12 double bond interacting with Cu^{2+}. The average Cu-H distance is about 3.23 Å which is slightly longer than that (3.16 Å) for the interaction with the middle double bond. The calculated IE (-1.78 kcal/mol) is smaller than that for the interaction with the middle double bond, suggesting that Cu^{2+} prefers to interact with the middle double bond. The convergences failed for the calculations of the interactions between other double bonds with Cu^{2+} probably due to the repulsion by the positively charged carbon. The charge distribution of **I** in the Cu^{2+}-**I** complex is different from **I** and the change is more significant for the middle four carbons. The negative charges on C14 and C14′ decrease by -0.037 and -0.040, respectively, and the negative charges on C15 and C15′ increase by 0.032 and 0.025, respectively, after the interaction, indicating that some negative charges on C14 and C14′ transfers to C15 and C15′, respectively. The calculations also show that **I** distorts slightly in the presence of Cu^{2+}. For example, the C14-C15=C15′-C14′ dihedral angle of **I** in the absence of Cu^{2+} is 179.64°, and 177.99 ° in the presence of Cu^{2+}.

To investigate how the conjugation length of an olefin affects the Cu^{2+}-olefin interaction, 1,3,5,7,9,11,13-tetradecaheptaene (**II**), Cu^{2+}-**II**, ethylene (**III**) and Cu^{2+}-**III** were calculated

by B3LYP, respectively. The optimized structures of **II**, Cu^{2+}-**II**, **III** and Cu^{2+}-**III** are shown in Fig. 5c, d, e and f, respectively. Different configurations of Cu^{2+}-**II** and Cu^{2+}-**I** complexes were examined in the calculations, the minimum structures of the complexes are shown in Fig. 5d and f, respectively. For **II**, the calculated interaction energies between Cu^{2+} and C1=C2, C3=C4, C5=C6 and C7=C8 double bonds are similar (-0.687, -0.688, -0.688 and -0.690 kcal/mol, respectively), suggesting that Cu^{2+} may interacts with any one of those double bonds. The middle double bond is chosen in this study. The calculated distances between Cu^{2+} and the two hydrogen atoms at the middle chain are almost the same. The average Cu-H distance is about 3.35 Å, which is longer than that (3.16 Å) for Cu^{2+}-**I** complex. This indicates that the interaction between Cu^{2+} and **II** is weaker than that between Cu^{2+} and **I**. For Cu^{2+}-**III**, the calculated four Cu-H distances are similar, and the average distance is about 2.97 Å. This indicates that the interaction between Cu^{2+} and **III** is relatively strong. To inspect how the conjugation lengths of the olefins affect the reorganization energies (REs) of the olefins and Cu^{2+}-complexes in the Cu^{2+}-olefin complexes and how the REs affect the interaction energies (IEs) between these species and Cu^{2+}, the REs and IEs were calculated for the three species. These are given in Fig. 6. The RE decreases significantly with the decrease of the conjugation length (or molecular size) from **I** to **II** to **III**. However, the C6-C7=C8-C9 dihedral angle of **II** in the Cu^{2+}-**II** complex is 177.46^{o}, which is smaller than the C14-C15=C15′-C14′ dihedral angle (177.99 ^{o}) of **I** in the Cu^{2+}-**I** complex. Although **I** is less distorted than **II** in the middle of the chain, the conjugation length of **I** is much longer than that of **II** (i.e. there are more dihedral angles, bonds and other angles in **I** than in **II**), which causes the RE of **I** is still larger than that of **II**. The less significant distortion of **I** is due to the hyperconjugation stabilization by the side chain methyl groups, otherwise the RE of **I** should be much larger. The IEs decrease in the order **III** > **I** > **II**, which is the same as the REs of the Cu^{2+}-complexes, indicating that the stronger interaction causes more distortion of the Cu^{2+}-complex. The decrease on IE in the Cu^{2+}-**II** complex is one order of magnitude larger than the increase in the RE with respect to that of **III**. Thus, this reduction on the IE in Cu^{2+}-**II** cannot totally attributed to the increase of RE of **II**, and other factors need to be considered. The total charges on the two carbons of **III** are -0.570 in the absence of Cu^{2+} and -0.606 in the presence of Cu^{2+}, and the total charges on the middle four carbons of **II** are

-0.494 in the absence of Cu^{2+} and -0.458 in the presence of Cu^{2+}. Thus the electrostatic interaction between Cu^{2+} and **III** is stronger than that between Cu2+ and **II**, which explains why the decrease on IE in the Cu^{2+}-**II** complex is one order of magnitude larger than the increase in the RE with respect to that of **III**. The fact that the IE of **I** is larger than that of **II** although the RE of **I** is larger than that of **II** can also be attributed to the stronger electrostatic interaction between Cu^{2+} and **I**. The calculated total charges on the middle four carbons of **I** are -0.636 in the absence of Cu^{2+} and -0.616 in the presence of Cu^{2+}, which are more negative than that of **II** (-0.494 in the absence of Cu^{2+} and -0.458 in the presence of Cu^{2+}). Thus, the electrostatic interaction between Cu^{2+} and **I** is stronger than that between Cu^{2+} and **II**. At long metal-olefin distance (> 3 Å), the orbital overlap extent between the metal and the olefin is very small, and the electrostatic interaction is probably stronger than other interactions. The average Cu-O bond lengths in the Cu^{2+}-**I**, Cu^{2+}-**II** and Cu^{2+}-**III** complexes are 1.923, 1.919 and 1.932 Å, respectively, suggesting that the stronger interaction causes longer Cu-O bond length. The Mulliken charge analysis shows that **I**, **II** and **III** in the complexes are stronger donors than acceptors. The net electron transfers from **I**, **II** and **III** to the Cu^{2+} complex are 0.055, 0.066 and 0.124, respectively. This suggests that the net electron donation from the olefins to the Cu^{2+}-complex increases with decreasing conjugation length.

For Cu^{2+}-**III**, the calculated Cu-H distance is 2.97 Å, which is much shorter than the calculated value (~3.7 Å) for **III** on the silica model surface. The interaction energy (~ -3.3 kcal/mol) on the MCM-41 surface is more than 10 times that (~ -0.3 kcal/mol) on silica surface, indicating that the different environments of Cu^{2+} affect the Cu^{2+}-olefin interaction significantly. This conclusion is consistent with the reported results[17,18] which show that the way to introduce Cu^{2+} onto the silica surfaces affect the Cu^{2+}-**III** interaction significantly. This conclusion should have practical applications in many fields, such as catalyst design, chromatographic separation, etc. Further study will be carried out to understand why the different environments of Cu^{2+} affect the Cu^{2+}-olefin interaction significantly, and what type of environment favors the Cu^{2+}-olefin interaction.

Conclusions

This study shows that B3LYP/6-311+G(d) with BSSE correction is suitable for the DFT study of the interaction between olefins and Cu^{2+} on silica and MCM-41 model surfaces. The all electron basis set 6-311+G(d) performs better than the popular mixed basis set 6-311+G(d) + LANL2DZ (on Cu) by ~0.4 Å in the prediction of Cu-H distances. The reorganization energy of an olefin in the presence of Cu^{2+} increases with increasing conjugated chain length (or molecular size). The distortion of an olefin can be reduced by hyperconjugation stabilization. The interaction energy between Cu^{2+} and the olefin is related to the reorganization energy of the olefin and the electrostatic interaction between Cu^{2+} and the olefin. The net electron donation from the olefins to Cu^{2+} on MCM-41 surface increases with decreasing conjugation length. The DFT calculation of the charge distribution of an olefin can be used to determine which double bond of the olefin may interact with the metal ion due to electrostatic attraction. The most important conclusion of this study is that the different environments of Cu^{2+} affect the Cu^{2+}-olefin interaction significantly, and the interaction energy on the MCM-41 surface is more than 10 times that on silica surface. This conclusion is not only supported by the experiments, but also confirmed by the calculations.

References

(1) *Metal-catalysis in Industrial Organic Processes*; G. P. Chiusoli and P. M. Maitlis, Eds.; RSC Publishing: London, 2008.

(2) R. H. Crabtree, *The Organometallic Chemistry of Transition Metals*, 4th ed.; Wiley: New York, 2005.

(3) S. Bhaduri and D. Mukesh, *Homogeneous Catalysis: Mechanisms and Industrial Applications*; Wiley: New York, 2000.

(4) G. W. Parshall and S. D. Ittel, *Homogeneous Catalysis: The Applications and Chemistry of Catalysis by Soluble Transition Metal Complexes*, 2nd ed.; Wiley: New York, 1992.

(5) C. Elschenbroich and A. Salzer, *Organometallics: A Concise Introduction*, 2nd ed.; VCH: Weinheim, 1992.

(6) J. P. Collman, L. S. Hegedus, J. R. Norton and R. G. Finke, *Principles and Applications of Organotransition Metal Chemistry*, University Science Books: Mill Valley, CA, 1987.

(7) M. J. S. Dewar, *Bull. Chem. Soc. Fr.* 1951, **18**, C71.

(8) J. Chatt and L. A. Duncanson, *J. Chem. Soc.* 1953, 2939.

(9) R. A. Love, T. F. G. Koetzle, J. B Williams and L. C Andrews, Bau, R. Inorg. Chem., 1975, **14**, 2653.

(10) D. L. Cedeño and E. Weitz, J. Am. Chem. Soc. 2001, **123**, 12857.

(11) D. L. Cedeño, E. Weitz and A. Bérces, *J. Phys. Chem. A*, 2001, **105**, 8077.

(12) D. N. Schlappi and D. L.Cedeño, *J. Phys. Chem. A*, 2003, **107**, 8763.

(13) D. L. Cedeño and R. Sniatynsky, *Organometallics*, 2005, **24**, 3882.

(14) D. N. Schlappi and D. L. Cedeño, *J. Phys. Chem. A*. 2009, **113**, 9692.

(15) (a) A. Poater, X. Solans-Monfort, E. Clot, C. Cope´ret and O. Eisenstein, *J. AM. CHEM. SOC.* 2007, **129**, 8217. (b) F. Bernardi, A. Bottoni and G. Pietro Miscione, *Organometallics* 2003, **22**, 940, (c) A. C. Tsipis *Organometallics* 2010, **29**, 354.

(16) (a) M. Kertesz, C. H. Choi and S. J. Yang, *Chem. ReV.* 2005, **105**, 3448. (b) F. Terstrgen,

and V. Buss, *J. Mol. Struct.* (*THEOCHEM.*) 1998, **430**, 209.

(17) T. Ichlkawa, H. Yorhlda and L. Kevan, *J. Phys. Chem.* 1982, **86**, 881.

(18) M. Narayana, R. Y. Zhan and L. Kevan, *J. Phys. Chem.* 1984, **88**, 3990.

(19) Y. Gao, L. D. Kispert, J. van Tol and L.-C. Brunel, *J. Phys. Chem. B* 2005, **109**, 18289.

(20) T. Ichikawa, H. Yoshida and L. Kevan, *J. Chem. Phys.* 1981, **75**, 2485.

(21) P. Pietrzyk, *J. Phys. Chem. B* 2005**, 109**, 10291.

(22) A. Rimola, D. Costa, M. Sodupe, L.-F. Lambert and P. Ugliengo, *Chem. Rev.*, Article ASAP.

(23) Y Gao, T. A Konovalova, J. N. Lawrence, M. A. Smitha, J; Nunley, R. Schad and L. D. Kispert, *J. Phys. Chem. B* 2003, **107**, 2459.

(24) M. J. Frisch, G. W. Trucks, H. B. Schlegel, G. E. Scuseria, M. A. Robb, J. R. Cheeseman, G. Scalmani, V. Barone, B. Mennucci, G. A. Petersson, H. Nakatsuji, M. Caricato, X. Li, H. P. Hratchian, A. F. Izmaylov, J. Bloino, G. Zheng, J. L. Sonnenberg, M. Hada, M. Ehara, K. Toyota, R. Fukuda, J. Hasegawa, M. Ishida, T. Nakajima, Y. Honda, O. Kitao, H. Nakai, T. Vreven, J. A. Montgomery, Jr., J. E. Peralta, F. Ogliaro, M. Bearpark, J. J. Heyd, E. Brothers, K. N. Kudin, V. N. Staroverov, R. Kobayashi, J. Normand, K. Raghavachari, A. Rendell, J. C. Burant, S. S. Iyengar, J. Tomasi, M. Cossi, N. Rega, J. M. Millam, M. Klene, J. E. Knox, J. B. Cross, V. Bakken, C. Adamo, J. Jaramillo, R. Gomperts, R. E. Stratmann, O. Yazyev, A. J. Austin, R. Cammi, C. Pomelli, J. Ochterski, R. L. Martin, K. Morokuma, V. G. Zakrzewski, G. A. Voth, P. Salvador, J. J. Dannenberg, S. Dapprich, A. D. Daniels, O. Farkas, J. B. Foresman, J. V. Ortiz, J. Cioslowski and D. J. Fox, GAUSSIAN 09 (Revision A.02), Gaussian, Inc.,

Wallingford, CT, 2009.

(25) A. D. Becke, *Phys. Rev. A: At., Mol., Opt. Phys.* 1988, **38**, 3098.

(26) J. P. Perdew and W. Yue, *Phys. Rev. B* 1986, **33**, 8800.

(27) J. P. Perdew, K. Burke and M. Ernzerhof, *Phys. Rev. Lett.* 1996, **77**, 3865.

(28) J. P. Perdew, K. Burke and M. Ernzerhof, *Phys. Rev. Lett.* 1997, **78**, 1396.

(29) A. D. Becke, *J. Chem. Phys.* 1993, **98**, 5648.

(30) J. M. Tao, J. P. Perdew, V. N. Staroverov and G. E. Scuseria, *Phys. Rev. Lett.* 2003, **91**, 146401.

(31) S. Grimme, *J. Comput. Chem.* 2006, **27**, 1787.

(32) A. D. Becke, *J. Chem. Phys.* 1997, **107**, 8554.

(33) Y. Zhao and D. G. Truhlar, *Theor. Chem. Acc.* 2008, **120**, 215.

(34) Y. Zhao and D. G. Truhlar, *Acc. Chem. Res.* 2008, **41**, 157.

(35) T. Yanai, D. Tew and N. Handy, *Chem. Phys. Lett.* 2004, **393**, 51.

(36) S. F. Boys and F. Bernardi, *Mol. Phys.* 1970, **19**, 553.

(37) N. N. Vlasova, Colloid Surf. A-Physicochem. Eng. Asp. 2000, **163**, 125.

(38) P. J. Hay and W. R. Wadt, *J. Chem. Phys.* 1985, **82**, 299.

(39) Y. Yang, N. W. Weaver and M. M. Kenneth, *J. Phys. Chem. A. 2009,* **113**, 9843.

(40) T. H. Jr. Dunning, *J. Chem. Phys.* 1989, **90**, 1007.

(41) D. E. Woon and T. H. Jr. Dunning, *J. Chem. Phys.* 1993, **98**, 1358.

Chart 1

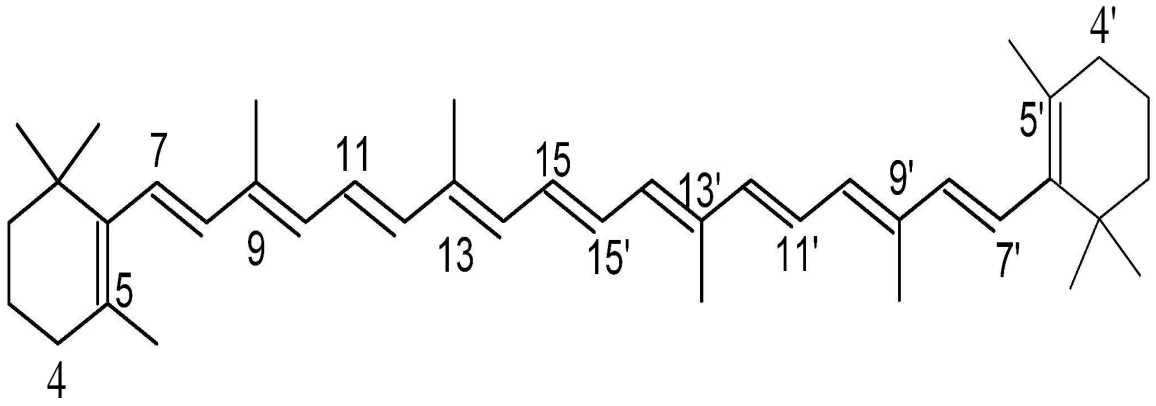

all-*trans* β-carotene（**I**）

Figure captions

Figure 1. (a) The model for Cu^{2+} on a silica surface optimized by B3LYP/6-311+G(d,p), (b) the optimized structure of the Cu^{2+}-C_2H_4 complex by B3LYP/6-311+G(d,p) and (c) the optimized structure of the Cu^{2+}-C_2H_4 complex by B3LYP/6-311+G(d,p) with the BSSE correction. H: light gray, O: red, Cu: orange and C: dark gray.

Figure. 2. The Cu-H distances calculated by the nine functionals using basis set 6-311+G(d,p) and the mixed basis set 6-311+G(d,p)+LANL2DZ, and the Cu-D distance measured by ESEM is also shown in the figure for comparison.

Figure 3. The bond length of Cu-O1 (a) and that of Cu-O2 (b) before and after the interaction calculated with the nine functionals using 6-311+G(d,p) basis set.

Figure 4. The calculated interaction energy (IE) between C_2H_4 and Cu^{2+} by B3LYP using 6-311+G(d,p), 6-311++G(2d,2p), 6-311++G(3d,3p), 6-311++G(df,pd) and aug-cc-pVTZ with and without the BSSE correction.

Figure 5. The optimized structures of **I** (a), Cu^{2+}-**I** (b), **II** (c), Cu^{2+}-**II** (d), **III** (e) and Cu^{2+}-**III**(f). **I**, **II** and **III** are calculated by B3LYP/6-31G(d) and the Cu^{2+}-olefin complexes are calculated by B3LYP with the BSSE correction using the mixed basis set (6-311+G(d) for Cu, 6-31G(d) for **I**, **II** and **III**, and the three oxygen atoms coordinated to Cu^{2+}, and 3-21G for the remaining atoms). H: light gray, O: red, Cu: orange and C: dark gray. Si: blue-gray.

Figure 6. The calculated REs of olefins and Cu^{2+}-complexes and IEs.

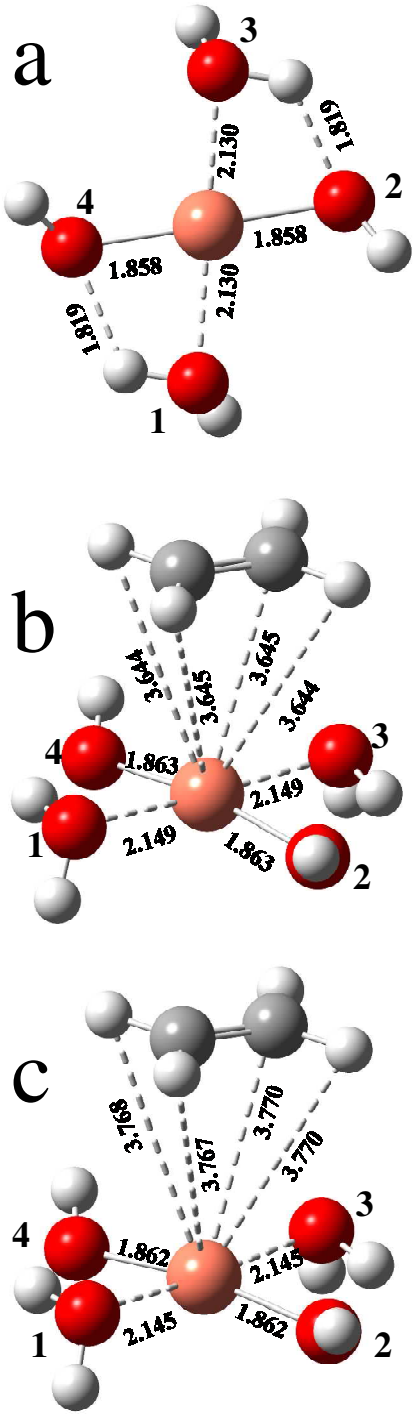

Fig. 1

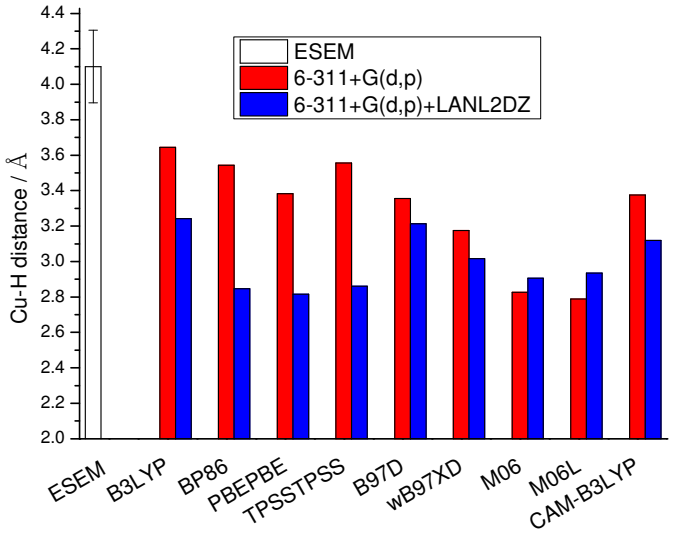

Fig. 2

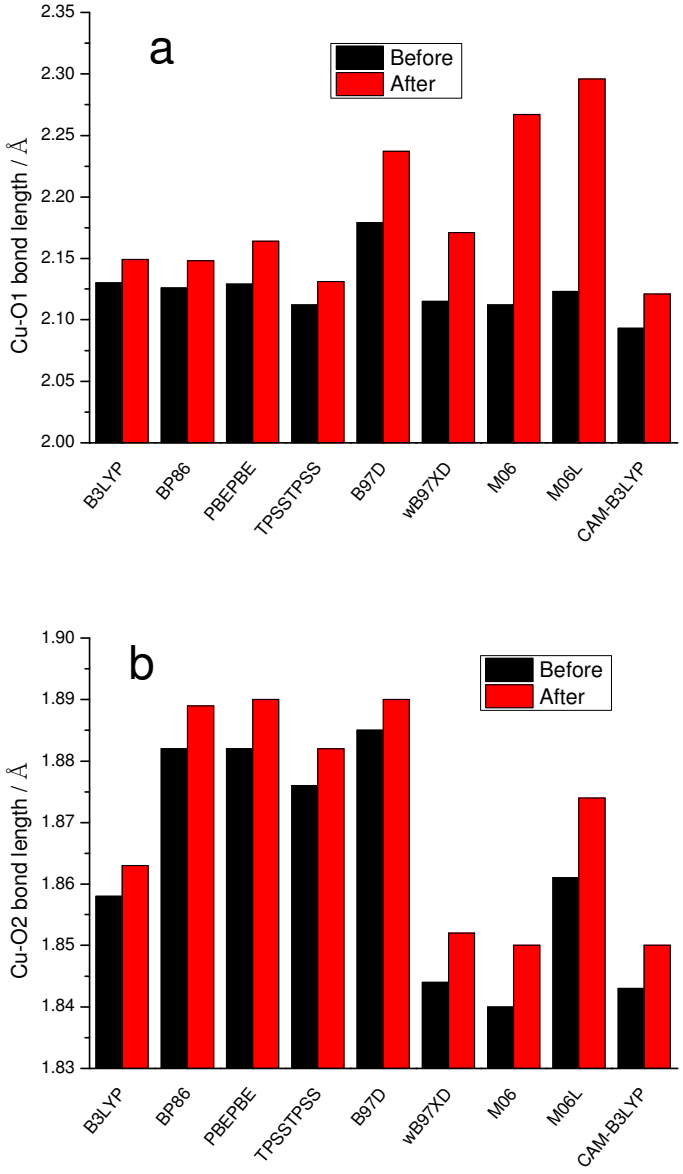

Fig. 3

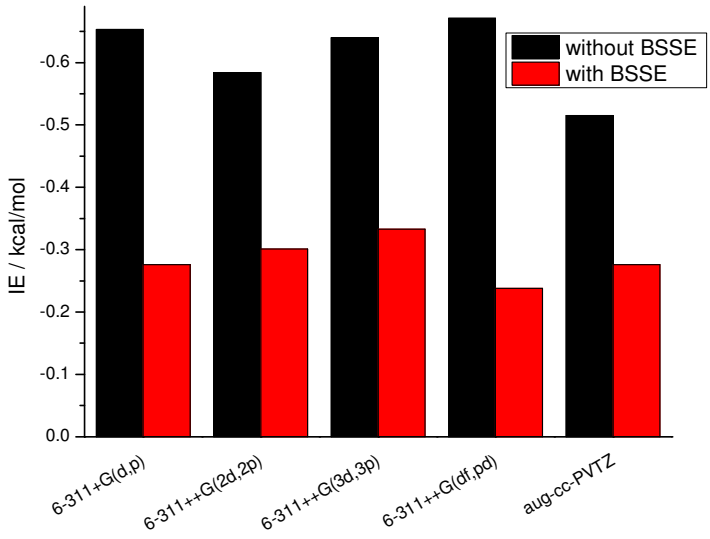

Fig. 4

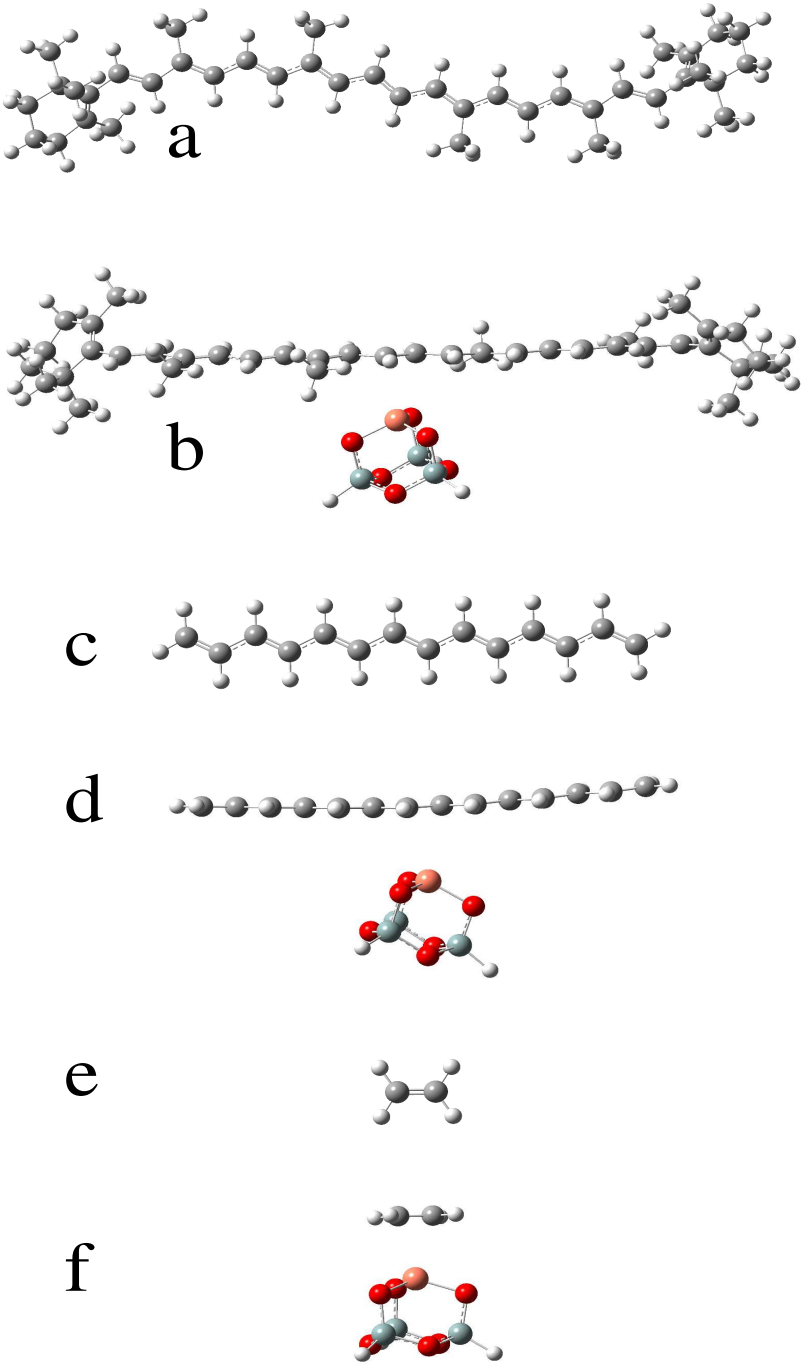

Fig. 5

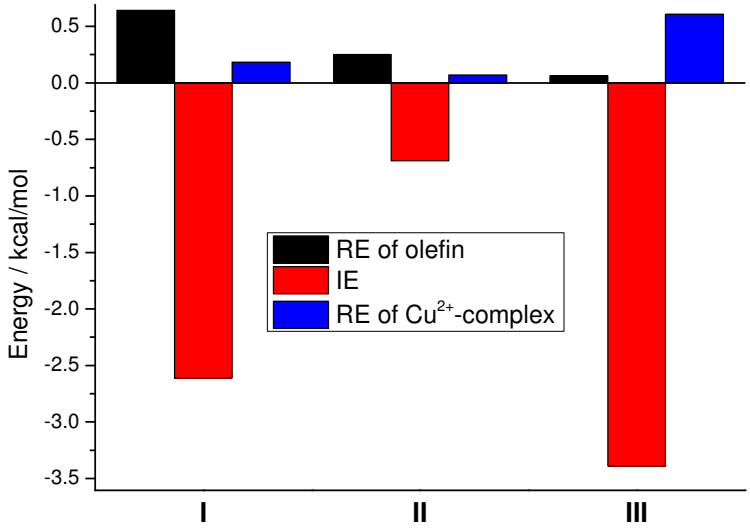

Fig. 6

Table 1. The charge distribution of **I**

C5	C6	C7	C8	C9	C10	C11	C12	C13	C14	C15
0.099	0.090	-0.214	-0.147	0.176	-0.192	-0.127	-0.175	0.180	-0.198	-0.120

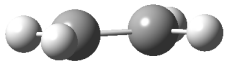

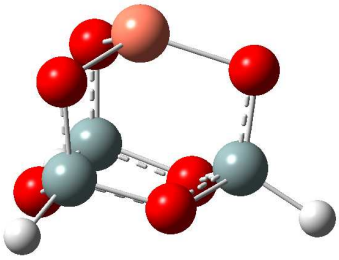

The conjugation length of an olefin and the environment of Cu^{2+} affect Cu2+-olefin interaction significantly